DRUG DISCOVERY

To Cite:
Afolayan FID, Ibrahim S. Computational simulations of phytoconstituents derived from *Phyllanthus amarus* against *Plasmodium falciparum* molecular targets. *Drug Discovery* 2023; 17: e26dd1937
doi: https://doi.org/10.54905/disssi.v17i39.e26dd1937

Author Affiliation:
Cell Biology and Genetics Unit, University of Ibadan, Nigeria

*Corresponding author
Cell Biology and Genetics Unit, University of Ibadan, Nigeria
Email: fidifede@gmail.com

Peer-Review History
Received: 29 March 2023
Reviewed & Revised: 02/April/2023 to 08/June/2023
Accepted: 12 June 2023
Published: 15 June 2023

Peer-Review Model
External peer-review was done through double-blind method.

Drug Discovery
pISSN 2278–540X; eISSN 2278–5396

Computational simulations of phytoconstituents derived from *Phyllanthus amarus* against *Plasmodium falciparum* molecular targets

Afolayan FID*, Ibrahim S

ABSTRACT

There has been an increase in the resistance of plasmodium parasites to already available malaria prevention drugs. Hence, the need for novel malaria-preventive medications. This study identified potential antiplasmodial drug candidates from *Phyllanthus amarus*. The phytoconstituent of *Phyllanthus amarus* was discovered using the Indian Medicinal Plants, Phytochemistry and Therapeutics Database as well as Dr Duke's phytochemical and ethnobotanical databases. The compounds were screened for ADMET properties and docked with five validated drug targets of *Plasmodium falciparum* using PyRx software. The molecular dynamics of the best complexes were simulated using Desmond software. A total of 54 compounds were retrieved for *Phyllanthus amarus* from the databases. Out of the 54 compounds, 26 were druggable, of which the majority showed a good ADMET profile. Amarulone - *P. falciparum* thioredoxin reductase (4b1b), Amarulone - *P. falciparum* enoyl-acyl carrier protein Reductase, Amariin-4b1b and Amarulone - *Plasmodium falciparum* lactate dehydrogenase (1u5c) complexes had the lowest binding energies of -12.3, -11.6, -11.3 and -11.2 kcal/mol, respectively. Amarulone-1u5c complex showed the lowest average RMSD value of 1.86 and 2.02 Å for the heavy backbone and protein-ligand complex, respectively. This makes the complex the most stable complex. Hence, further research should be done on Amarulone as a malaria drug candidate.

Keywords: *Plasmodium falciparum*, drug targets, molecular docking, *Phyllanthus amarus*, molecular dynamics.

1. INTRODUCTION

The parasite *Plasmodium species* is the primary cause of malaria. Female Anopheles mosquitoes carrying the Plasmodium parasite are the primarily responsible for the deadly disease. In Africa and other tropical and subtropical regions of the world, it is the most common protozoan-borne parasitic disease (Makenga et al., 2020). Four different species of plasmodium are the main causes of malaria. These are *P. malariae*, *P. vivax*, *P. falciparum* and *P. ovale*. Among the

four species of plasmodium mentioned, the most harmful strain of malaria in the world is caused by *P. falciparum* (Rout and Mahapatra, 2019).

In recent times, there has been progressively more malaria cases reported worldwide. This has been implicated in the malaria parasite's resistance to the available antimalarial drugs artemisinin (Birnbaum et al., 2017). Hence, the search for novel malaria medications is becoming more and more important. Fortunately, the *in silico* approach is fast becoming an indispensable method in drug discovery studies by estimating the biological effect of phytoconstituents against therapeutic targets. Predicting the interactions of small compounds with protein targets has been made possible by techniques like molecular docking, molecular dynamics simulation and ADMET screening.

Also, the computational approach has been handy in evaluating the physicochemical parameters of the molecules in regard to their structural and molecular configurations. More so, contrary to the conventional method, adopting the dry-lab (*in silico*) approach has been shown to reduce costs and time while also improving the drug development process. For the creation of new malaria therapies, *P. falciparum* lactate dehydrogenase (pfLDH) is a crucial molecular pharmacological target. It is an enzyme that serves as a catalyst in the reversible conversion of pyruvate to lactate using NAD^+ as a co-factor in glycolysis (Shadrack et al., 2016).

Without this enzyme, *P. falciparum* will not be able to generate the energy needed for growth, metabolic processes and development (Shadrack et al., 2016). This shows that inhibition of this enzyme will result in the parasite demise (Chaniad et al., 2021). For this reason, some potential antimalarial drugs have been designed to target *Pf*LDH enzyme (Chaniad et al., 2021; Shadrack et al., 2016).

Most antifolate antimalarial drugs such as pyrimethamine and proguanil interfere with folate metabolism, a pathway necessary for the survival of malaria parasite. These drugs work by inhibiting two important enzymes: dihydrofolate reductase (DHFR) (pyrimethamine, cycloguanil) and dihydropteroate synthase (DHPS) (sulfadoxine), which are responsible for *de novo* biosynthesis of folate. Inhibiting this metabolic process will prevent the manufacture of amino acids, pyrimidines and purines, which will then prevent DNA synthesis and cause parasite cell death (Singh and Mishra, 2018).

This shows that *P. falciparum* dihydrofolate reductase-thymidylate synthase (*Pf*DHFR-TS) is a crucial enzyme that is indispensable to *P. falciparum*. Also, *Pf*DHFR is significantly divergent from the human DHFR (hDHFR) as both enzymes differ in sequence and in structure. The sequences of the hDHFR and PfDHFR enzymes align at 33% of the residues and are only 20% similar (Sharma et al., 2017). Furthermore, while PfDHFR is encoded on the same polypeptide chain as the TS enzyme, human TS and DHFR are encoded by two distinct and separate enzymes. Hence, the bifunctional *Pf*DHFR-TS are thus a suitable and validated molecular target for the creation of cutting-edge malaria drugs drug.

Fatty acid synthase (FAS) is needed for the production of the fatty acids (FAs) that are required for the formation of the parasite cell membrane known as the parasitophorous vacuole. This enables the parasite to live longer in the host and protects it against the host cell's immune response. Early studies suggested that *Plasmodium* relies only on exogenous FAs from the host (Elabbadi et al., 1992). However, this was disproved Ralph et al., (2004) found FAS machinery in the apicoplast. New biological synthesis of FAS is also as important because the liver stage of *Plasmodium* can't survive without it (Vaughan et al., 2009). When it comes to membrane biogenesis in the blood stage, exogenous FAs are sufficient (Qidwai and Khan, 2012).

Disruption of *P. falciparum* FAS can be achieved by targeting enoyl-acyl carrier protein reductase (ENR), which is a rate-limiting enzyme in FAS biosynthesis (Costa-Júnior et al., 2022). *Plasmodium falciparum* ENR (*Pf*ENR) is responsible for reducing the trans-2-enoyl bond of enoyl-acyl carrier protein (ACP) substrate to saturated acyl-ACPs using NADH as a cofactor (Narayanaswamy et al., 2017). Hence, it is responsible for the catalysis of the final reaction in the FAS-II pathway, which makes it an ideal target for novel antimalarial medication development.

The reduction of thioredoxin is catalyzed by thioredoxin reductase, which is a vital part of the thioredoxin system (Bjørklund et al., 2021). Thioredoxin reductase (TrxR), its substrate thioredoxin (Trx) and NADPH work together in *P. falciparum* to lessen oxidative stress and keep the parasite's redox balance stable (Jortzik and Becker, 2012). Thus, it shields the parasite against reactive oxygen species (ROS) during its crucial erythrocytic phase, which is necessary for its survival. *Plasmodium falciparum* Thioredoxin Reductase (PfTrxR) C-terminal cysteines (as a cystine participates in catalysis via an intramolecular dithiol-disulfide interchange with the growing redox-active dithiol (O'Keefe et al., 2018).

Plasmodium falciparum Thioredoxin reductase (PfTrxR) is thus a suitable target for the development of novel anti-malarial drugs. The fourth enzyme in the new uridylate synthesis, *P. falciparum* dihydroorotate dehydrogenase, accelerates the conversion of dihydroorotate to orotate through an enzymatic process akin to ping-pong. The parasite will perish if this enzyme is inhibited because it requires pyrimidines for the synthesis of DNA and other activities. Consequently, this enzyme is a crucial molecular medicinal target (Hoelz et al., 2018).

The plant *Phyllanthus amarus* (*P. amarus*) is a member of the Phyllanthaceae family. It is commonly referred to as Windbreaker or Gale of Wind in English. In Nigeria, it is referred to by various names such as "Ebebenizo" in Bini "Ehin Olobe" in Yoruba, (Etta, 2008), "Ngwu" by the Igbo tribe, "Buchi oro" by the Asaba people and Mache Dagooyo in Hausa. *P. amarus* is a popular perennial herb that has been used for more than 2000 years in Ayurvedic medicine. It has been used in the treatment of a wide range of ailments and disorders (Adjene and Nwose, 2010). Several studies have also shown its antimalarial activity.

In a study conducted by Aliyu et al., (2021) using various extracts of *P. amarus* against *P. falciparum*, it was observed that *P. amarus* shows excellent antimalarial activity against *P. falciparum* isolates *in vitro.* Donkor et al., (2015) also noticed an equivalent outcome, where *P. amarus* also show good antimalarial activity against *P. falciparum*. However, the compounds responsible for the antiplasmodial activity of *P. amarus* are yet to be determined. Therefore, this study aims to investigate the druggability, inhibitory potential and activities of phytoconstituent derived from *Phyllanthus amarus* on *Plasmodium falciparum* molecular targets via molecular docking and molecular dynamics simulation.

2. MATERIALS AND METHODS

Mining of Phytoconstituents

The phytochemicals in *Phyllanthus amarus* were collected from Dr Duke's Phytoconstituent and Ethnobotanical Databases (https://phytochem.nal.usda.gov/phytochem/search/list) and the Indian Medicinal Plants, Phytochemistry and Therapeutics Database (IMPPAT, https://cb.imsc.res.in/imppat/basicsearchauth) (Mohanraj et al., 2018). The phytoconstituents were retrieved from the databases by searching the database using the plant's botanical name.

Drug likeness Predictions of Ligands using Lipinski's Rule of Five

For drug likeness prediction, the canonical smiles format of the ligands was mined from PubChem database https://pubchem.ncbi.nlm.nih.gov/. These SMILES were then queried in the molsoft (http://molsoft.com/mprop/) web tool. In accordance with Lipinski's rule of five, Molsoft determines the drug-likeness score of each phytoconstituent (Lipinski, 2004).

ADMET Prediction

Ames mutagenesis, eye irritation, CYP3A4, CYP1A2, CYP2C9 and CYP2D6 inhibition, blood-brain barrier permeability, human oral bioavailability, sub-cellular localization and hepatotoxicity were all predicted using admetSAR2.0 Yang et al., (2019) using the ligands SMILES format.

Retrieval and Preparation of Ligands

The discovered phytoconstituents from *Phyllanthus amarus* in the Structure-data file (SDF) and three control ligands (Chloroquine, Artemether and Artesunate) were collected from PubChem database https://pubchem.ncbi.nlm.nih.gov/. The ligands were minimized and converted to pdbqt using PyRx (Dallakyan and Olson, 2015).

Retrieval and Preparation of Protein Targets

The PDB files for the five targets' three-dimensional structural (3D) conformers were mined from the RCSB protein databank http://rcsb.org (Desai and Joshi, 2019). The targets are: 1u5c (*P. falciparum* lactate dehydrogenase), 3lsy (*P. falciparum* enoyl-ACP reductase), 3sfk (*P. falciparum* dihydroorotate dehydrogenase), 4b1b (*P. falciparum* thioredoxin reductase) and 3dga (*P. falciparum* dihydrofolate reductase-thymidylate synthase).

Using the BIOVIA, (2020) Discovery studio (Discovery Studio, Release 2020) visualization tool, the water molecules and co-crystallized ligands connected to the protein were taken out before the energy minimization process and the output was archived in PDB format. The steepest descent method with a conjugate gradient step of 0.02 was applied to the targets using the Chimera tool UCSF 1.14 (Pettersen et al., 2004). The energy was minimized by employing the AMBER ff14SB force field, Gasteiger charges were distributed and hydrogen atoms were inserted as required.

Determination of Active Sites of Protein

The Computed Atlas for Surface Topography of Proteins (CASTp) service (http://sts.bioe.uic.edu/castp/index.html) was used to determine the amino acids present in the targets' active sites.

In silico Docking Studies

Using AutoDock Vina from PyRx, target proteins were docked with ligands and the binding affinities were evaluated (Dallakyan and Olson, 2015). Docking studies were performed on refined targets and 26 ligands.

Analysis of Ligand-Protein Interactions

Ligands are known to interact with their receptors' amino acid residue through hydrogen bonding and hydrophobic interaction. The best five complexes that displayed a high binding affinity with the targets, according to PyRx result, were chosen for ligand-protein interaction. These were viewed with BIOVIA, (2020) Discovery Studio software and PyMol software. The complex between each protein and compound was saved as a single file in pdb format. The interacting residues and the mode of interaction in each complex, hydrophobic interaction and hydrogen bonding were determined using the Ligplot+ tool (Laskowski and Swindells, 2011).

Molecular Dynamics Simulation

The top five complexes based on their binding affinities from the docking studies and the best complex among the control compounds were put through molecular dynamics (MD) simulations. Desmond software's Maestro-Desmond Interoperability tools were utilized to run the simulations, 2018. The top five hits are Amarulone-4b1b complex, Amarulone-3lsy complex, Amarulone-3dga complex, Amariin-4b1b complex and finally Amarulone-1u5c complex, while the best control compound with the highest binding activity is Artesunate-3sfk complex.

The docked ligand-receptor complexes were solvated in the TIP3P water model's orthorhombic box with 0.15 M NaCl, which was added to the system to add sodium ions (Na+) and balance the charges. The hit compounds were created using the OPLS3 force field. In all the simulations, the OPLS3 force field parameter was utilized (Harder et al., 2016). Using the default Desmond protocol, the system was relaxed. The long-range portion of the electrostatic interactions was calculated using the Particle Mesh Ewald (PME) approach, while the non-bonded electrostatic interactions were calculated through the M-SHAKE algorithm at the 9 cut-offs.

Utilizing the steepest descent technique for 50 000 steps in the initial energy reduction phase, the simulation then moved on to an equilibration step using NVT and NPT ensembles using Berendsen dynamics with a coupling constant of 12 ps at 10 K with a 2.0 fs time step and constraints on the solute non-hydrogen atoms. With and without constraints on the non-hydrogen atoms for intervals of 12 ps and 24 ps, respectively, the NPT ensemble performed the last steps of equilibration at 300K temperature.

The manufacturing step was then completed for 50 ns utilizing an NPT ensemble, a Nose-Hoover thermostat and a Martyna-Tuckerman-Klein barostat at 300 K and 1.0 atm using the Simulation Interaction Diagram (SID) tool included in the Desmond MD package, analysis of the behavior and interactions between ligands and enzymes were possible. The heavy backbone atoms' RMSD values and the ligand-protein complex's RMSD values were computed for the 50 ns simulation to confirm the stabilities of all the systems (Mosquera-Yuqui et al., 2022).

Post-Molecular Dynamics Simulation

Each protein-ligand complex was examined using post-MD analysis techniques such as root mean square deviation (RMSD) and root mean square fluctuation (RMSF). The complexes simulated are the Amariin-4b1b complex, Amarulone-1u5c complex, Amarulone-3dga complex, Amarulone-3lsy complex, Amarulone-4b1b complex and Artesunate-3sfk complex (Control).

3. RESULTS

Drug-likeness and ADMET Profile

The list of phytoconstituents, their molecular formulae, physicochemical properties and drug-likeness scores are in (Table 1). Out of the forty-six compounds screened, twenty-seven were druggable, that is, they have positive molsoft scores. The most drug-likeness was predicted for repandusinic acid B, with a score of 0.91.

The next step was to screen the Twenty-seven compounds with positive scores for their ADMET profiles. The results are in (Table 2). However, only six compounds are orally bioavailable, which are 4-O-Galloyl-quinic acid, Gallic-acid, Norsecurinine, Phyllanthin, Epibubbialine and 24isopropylcholesterol. Only compound 6 are carcinogenic and 50% of the compounds are mutagenic and hepatotoxic. Notably, Phytosterols, 24-isopropylcholesterol and l-ascorbic acid strictly abide by Lipinski's "rule of five" and theoretically passes the drug-likeness properties.

Table 1 Molecular formula, physicochemical properties and drug-likeness scores of phytoconstituents derived from *Phyllanthus amarus*

S/N	Phytochemical	Molecular formula (g/mol)	NHBA	NHBD	MolLogP	DLS
1	4-O-Galloyl-Quinic Acid	C14 H16 O10	10	7	-1.48	0.87
2	Amariin	C41 H28 O28	28	13	-1.52	0.49
3	Amarulone	C40 H26 O26	26	9	-0.33	0.14
4	Corilagin	C27 H22 O18	18	11	0.51	0.64
5	Epibubbialine	C12 H15 N O3	4	1	0.28	-0.67
6	Furosin	C27 H22 O19	19	10	-1.29	0.8
7	Gallic-Acid	C7 H6 O5	5	4	0.78	-0.22
8	Gallocatechin	C15 H14 O7	7	6	0.26	-0.04
9	Geraniin	C41 H28 O27	27	14	0.61	0.3
10	Hypophyllanthin	C24 H30 O7	7	0	3.67	0.81
11	Isoquercitrin	C21 H20 O12	12	8	-0.54	0.68
12	Norsecurinine	C12 H13 N O2	3	0	1.36	-1.44
13	Phyllanthin	C24 H34 O6	6	0	3.66	-0.56
14	Phyllanthine	C14 H17 N O3	4	0	1.26	-0.57
15	Repandusinic Acid B	C48 H34 O33	33	18	1.49	0.97
16	Rutin	C27 H30 O16	16	10	-1.55	0.91
17	Securinine	C13 H15 N O2	3	0	1.87	-1.22
18	Epibubbialine	C12 H15 N O3	4	1	0.28	-0.67
19	Fraternusterol	C28 H48 O2	2	1	7.01	-1.27
20	Phyllanthosecosteryl Ester	C53 H96 O4	4	2	16.01	0.55
21	Phyllanthosterol	C29 H50 O	1	1	8.95	0.54
22	Phytosterols	C29 H50 O	1	1	8.45	0.78
23	4methoxynorsecurinine	C13 H15 N O3	4	0	1.09	-0.99
24	24isopropylcholesterol	C30 H52 O	1	1	8.73	0.59
25	1-O,6-O-Digalloyl-Betad-Glucose	C20 H20 O14	14	9	-0.8	0.9
26	Astragalin	C21 H20 O11	11	7	-0.12	0.67
27	Dotriacontanoic Acid	C32 H64 O2	2	1	14.73	-0.54
28	Ellagic Acid	C14 H6 O8	8	4	1.53	-1.11
29	Estradiol	C18 H24 O2	2	2	3.61	0.63
30	Heptacosanoic Acid	C27 H54 O2	2	1	12.2	-0.54
31	Kaempferol	C15 H10 O6	6	4	1.61	0.5
32	L-Ascorbic Acid	C6 H8 O6	6	4	-1.59	0.74
33	Linolenic Acid	C18 H30 O2	2	1	5.88	0.09
34	Lintetralin	C23 H28 O6	6	0	3.6	0.37
35	Niranthin	C24 H32 O7	7	0	3.89	-0.19
36	Nirphyllin	C24 H32 O8	8	1	3.17	-0.53
37	Nirtetralin	C24 H30 O7	7	0	3.93	0.84
38	Nirurin	C32 H40 O15	15	9	1.02	0.82
39	Octadeca-9,12-Dienoic Acid	C18 H32 O2	2	1	6.6	-0.3
40	Phyllanthol	C30 H50 O	1	1	7.54	-0.16
41	Phyllnirurin	C20 H22 O5	5	1	3.83	0.02
42	Phyltetralin	C24 H32 O6	6	0	3.24	0.7
43	Quercetin	C15 H10 O7	7	5	1.19	0.52
44	Quercitrin	C21 H20 O11	11	7	0.32	0.82
45	Ricinoleic Acid	C18 H34 O3	3	2	5.67	-0.36
46	Vitamin P	C27 H30 O16	16	10	-1.55	0.91

NHBA- Number of hydrogen bond acceptors, NHBD- Number of hydrogen bond donors, DLS- Drug-likeness score

Table 2 The ADMET profiles of the Twenty-seven compounds that is druggable

S/N	Phytochemical	HIA.	Caco-2	BBB.	HOB	P-gylco.	CYP3A4	CYP2C9	CYP2D6	CYP1A2	Ames.	Hept.	Carc.
1	4-o-galloyl-quinic acid	0.9534	-0.8989	-0.369	0.6	-0.9339	-0.9167	-0.9325	-0.9462	-0.9108	-0.77	Yes	No
2	Amariin	0.8387	-0.8735	-0.3822	-0.5286	0.7494	-0.8235	-0.5802	-0.8388	-0.7992	0.62	Yes	No
3	Amarulone	0.8922	-0.8808	0.8937	-0.5286	0.7434	-0.7605	0.5905	-0.7792	-0.6916	0.56	Yes	No
4	Corilagin	0.8598	-0.9021	-0.7239	-0.5286	0.6416	-0.9116	-0.9083	-0.9575	-0.8596	-0.5	Yes	No
5	Furosin	0.7826	-0.8985	-0.2797	-0.6143	0.6924	-0.7601	-0.618	-0.8135	-0.7818	0.59	Yes	No
6	Geraniin	0.8387	-0.8798	-0.3822	-0.5	0.7459	-0.8235	-0.5802	-0.8388	-0.7992	0.64	Yes	Yes
7	Hypophyllanthin	0.9877	0.9093	0.9582	0.5714	0.8481	0.9175	0.8083	-0.533	-0.6867	-0.58	Yes	No
8	Isoquercitrin	0.6468	-0.901	-0.9152	-0.7286	-0.624	-0.9193	-0.9296	-0.9513	-0.9084	0.81	Yes	No
9	Repandusinic Acid B	0.7926	-0.8752	-0.8907	-0.5857	0.7305	-0.7552	-0.5938	-0.87	-0.7625	-0.5	Yes	No
10	Rutin	0.7322	-0.9269	-0.9393	-0.7429	-0.6165	-0.9249	-0.9071	-0.9545	-0.8673	0.8	Yes	No
11	Phyllanthosecosteryl Ester	0.9852	-0.8387	-0.9562	-0.6143	0.7251	-0.6578	-0.8508	-0.9301	-0.933	-0.83	No	No
12	Phytosterols	0.993	0.5385	0.9247	0.5286	-0.5	-0.8309	-0.9125	-0.9346	-0.9291	-0.87	No	No
13	24 isopropyl cholesterols	0.993	-0.5266	0.8569	0.6	-0.5181	-0.8638	-0.9194	-0.9519	-0.9355	-0.86	No	No
14	1-O,6-O-Digalloyl-Betad-Glucose	0.7734	-0.8814	-0.5362	-0.6	-0.5252	-0.8723	-0.7955	-0.9425	-0.9315	-0.69	No	No
15	Astragalin	0.6347	-0.9102	-0.9152	-0.7714	-0.612	-0.9193	-0.9296	-0.9513	-0.9084	0.62	Yes	No
16	Estradiol	0.9941	0.9313	-0.993	-0.9429	-0.9447	-0.8309	-0.939	-0.9574	0.9106	-0.98	No	No
17	Kaempferol	0.9881	-0.8637	-0.5635	-0.6286	-0.8576	0.7241	0.8948	-0.9083	0.9108	0.73	Yes	No
18	L-Ascorbic Acid	0.815	-0.9755	0.9785	0.5857	-0.9715	-0.9662	-0.9478	-0.9347	-0.8958	-0.94	No	No
19	Linolenic Acid	0.9087	0.6071	0.962	-0.5714	-0.8342	-0.9465	-0.8798	-0.9631	0.6915	-0.92	No	No
20	Lintetralin	0.9877	0.9281	0.9618	-0.6429	0.8423	0.9382	0.823	0.5325	-0.5844	0.55	Yes	No
21	Nirtetralin	0.9877	0.9114	0.9582	-0.6	0.8213	0.9175	0.8083	-0.533	-0.6867	-0.52	Yes	No
22	Nirurin	0.7981	-0.8891	-0.8127	-0.8	-0.5423	-0.9436	-0.6518	-0.7932	-0.5844	-0.66	Yes	No
23	Phyllnirurin	0.9788	0.8649	0.949	-0.6286	0.6376	0.656	0.5066	-0.6878	-0.5398	-0.56	Yes	No
24	Phyltetralin	0.9958	0.918	0.9426	0.5286	0.8584	0.6931	0.5249	-0.881	0.6213	-0.63	Yes	No
25	Quercetin	0.9833	-0.6417	-0.4632	-0.5429	-0.9191	0.6951	-0.5823	-0.9287	0.9106	0.9	Yes	No
26	Quercitrin	0.7322	-0.7858	-0.585	-0.6857	-0.5351	-0.7109	-0.8538	-0.9547	-0.5306	0.77	Yes	No
27	Vitamin P	0.7322	-0.9269	-0.9393	-0.7429	-0.6165	-0.9249	-0.9071	-0.9545	-0.8673	0.8	Yes	No

HIA. = Human Intestinal absorption, HBB. = Blood brain barrier, HOB = Human oral bioavailability,
P-gylco. = P-glycoprotein inhibitor, Ames. = Ames mutagenesis, Hept. = Hepatotoxicity, Carc. = Carcinogenicity

In silico Docking Studies

The binding energies (ΔG (kcal/mol)) of the compounds identified in Phyllanthus amarus as calculated by PyRx are in (Table 3). The majority of the compounds demonstrated good binding affinities with the molecular drug targets while others did not perform well. The binding energies range from -12.3 to 22.5 kcal/mol.

The five complexes with the best binding affinities are Amarulone-4b1b (*P. falciparum* Thioredoxin Reductase) at ΔG= −12.3 kcal/mol; Amarulone-3lsy (*P. falciparum* Enoyl-ACP Reductase) at ΔG= −11.6 kcal/mol; Amarulone-3dga (*P. falciparum* dihydrofolate reductase-thymidylate synthase) at ΔG= −11.3 kcal/mol; Amariin-4b1b (*P. falciparum* Thioredoxin Reductase) at ΔG= −11.3 kcal/mol and Amarulone-1u5c (*P. falciparum* lactate dehydrogenase) at ΔG= −11.2 kcal/mol as in (Figure 1a, 2a, 3a, 4a, 5a). These compounds perform extremely well when compared with the standards (artemether-3dga = -8.6 kcal/mol, artesunate-3lsy = -8.6 kcal/mol, artemether-3lsy = -8.6 kcal/mol, artesunate-3sfk = -9.9 kcal/mol, artemether-3sfk = -9.3 kcal/mol,).

Table 3 PyRx docking outcomes for the phytocompounds of *Phyllanthus amarus* with *Plasmodium falciparum* molecular drug target

Phytochemical	ΔG (kcal/mol)				
	1u5c	3dga	3lsy	4b1b	3sfk
4-o-galloyl-quinic acid	-7.4	-8.5	-8.1	-7.5	-9.6
Amariin	-9.7	-10	-8	-11.3	-7.8
Amarulone	-11.2	-11.3	-11.6	-12.3	-7
Corilagin	-9.1	-8.4	-9.2	-9.6	-8
Furosin	-9.2	-9.4	-8.3	-9.8	-8.9
Geraniin	-10.4	-10.3	-8.7	-9.8	-7.3
Hypophyllanthin	-6.5	-8.7	-6.8	-6.9	-7.3
Isoquercitrin	-7.9	-9.1	-9.6	-8.4	-10.7
Repandusinic acid b	-10	-11	-9	-10.9	-7.5
Rutin	-8.4	-7.9	-10.7	-8.6	-7.8
Phyllanthosecosteryl ester	-6.1	-5.4	-6.5	-8.1	-8.6
Phytosterols	-8.3	-9.9	-9.3	-8.1	-7.6
24isopropylcholesterol	-8.7	-9.8	-9.3	-8.2	-7
1,6-Bis-O-galloyl-beta-D-glucose	-8.2	-8.7	-8.1	-8.3	-8.1
Astragalin	-7.5	-8.8	-8.9	-7.9	-8.9
Estradiol	-8.3	-8.6	-9.3	-7.8	-9.3
Kaempferol	-7.2	-8.3	-8.7	-7.6	-8.7
L-ascorbic acid	-5	-6.3	-5.2	-6.3	-5.2
Linolenic acid	-5.3	-5.9	-6.5	-5.6	-6.5
Lintetralin	-6.6	-8.3	-8	-7.5	-8
Nirtetralin	-6.7	-6.7	-6.9	-6.8	-6.9
Nirurin	-9.5	-8.7	-8.6	-9.7	-8.6
Phyllnirurin	-8.2	-8.8	-8.8	-7.7	-8.8
Phyltetralin	-6.2	-7.5	-6.9	-6.5	-6.9
Quercetin	-7.3	-8.4	-8.8	-8.9	-8.8
Quercitrin	-8.1	-7.9	-9.4	-8.4	-9.4
*Artemether	-6.7	-8.6	-8.6	-7.4	-9.3
*Chloroquine	-6.2	-6.6	-7.6	-5.6	-8.1
*Artesunate	-8.1	-7.3	-8.6	-8.2	-9.9

*Standard drugs (Control), *P. falciparum* lactate dehydrogenase (1u5c), *P. falciparum* dihydrofolate reductase-thymidylate synthase (3dga), *P. falciparum* Enoyl-ACP Reductase (3lsy), *P. falciparum* dihydroorotate dehydrogenase (3sfk) and *P. falciparum* Thioredoxin Reductase (4b1b)

Analysis of Ligand-Protein Interactions

Figure 1b, 2b, 3b, 4b, 5b show the type of interaction and bond distance between the ligands and the targets of the best-docked compounds. The amino acid residues of 4b1b (*Pf*TrxR) to which the most active inhibitors (Amarulone) form hydrogen bonds are Asn 336, Lys338, Ile393 and Gly407. The second most active compound Amariin also forms hydrogen bond with some of the amino acid residues that Amarulone bonded with such as Asn 336, Lys338, Gly407.

Other amino acids Amariin formed a hydrogen b with are Ala 230 and Asn 361. While, in the interaction of the most active compound (Amarulone) with 3lsy (*Pf*ENR) as shown in Figure 2b, Phe421 is the only amino acid that forms a hydrogen bond with Amarulone, all other amino acids form hydrophobic contact with Amarulone. These amino acids are Pro275, Gly276, Tyr267/371/375, Val274, Leu417, His268, Asn418 and Met420.

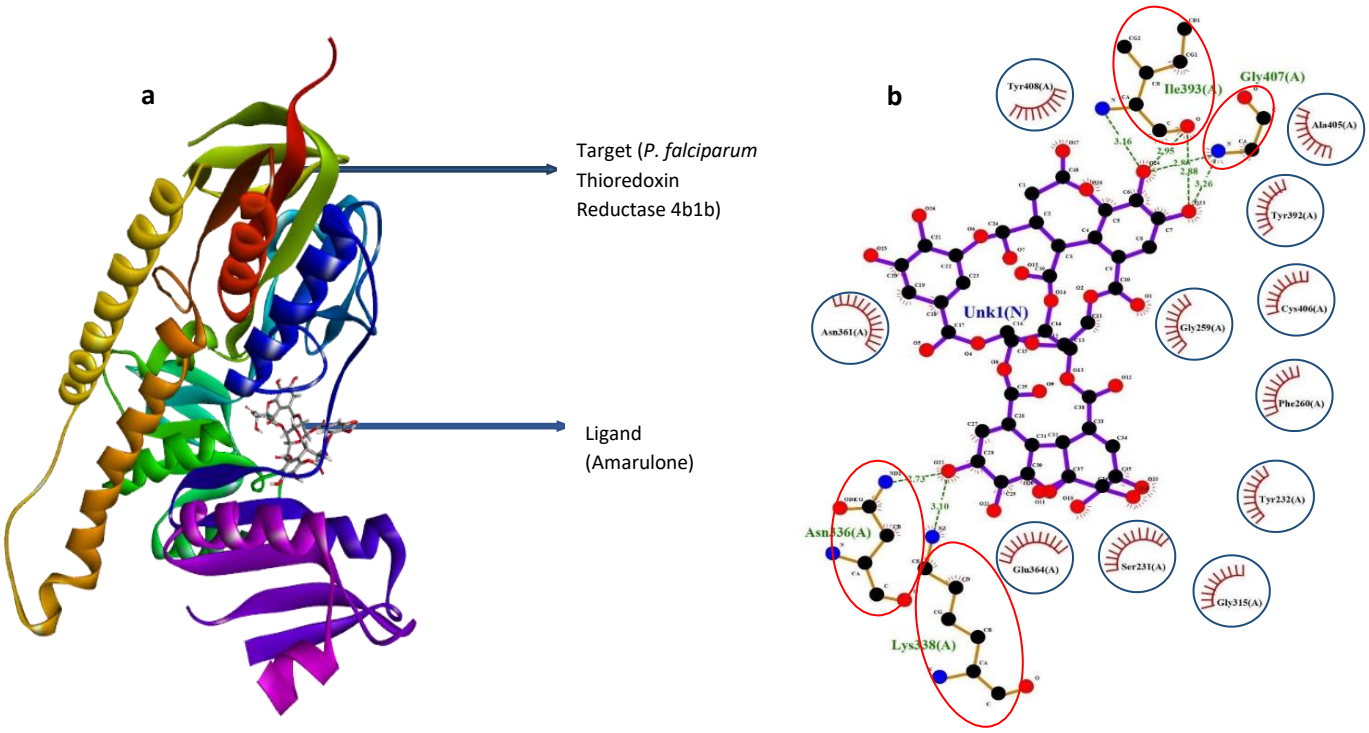

Figure 1 Amarulone-4b1b docked complex, showing interaction between the ligand and protein and the binding site residue

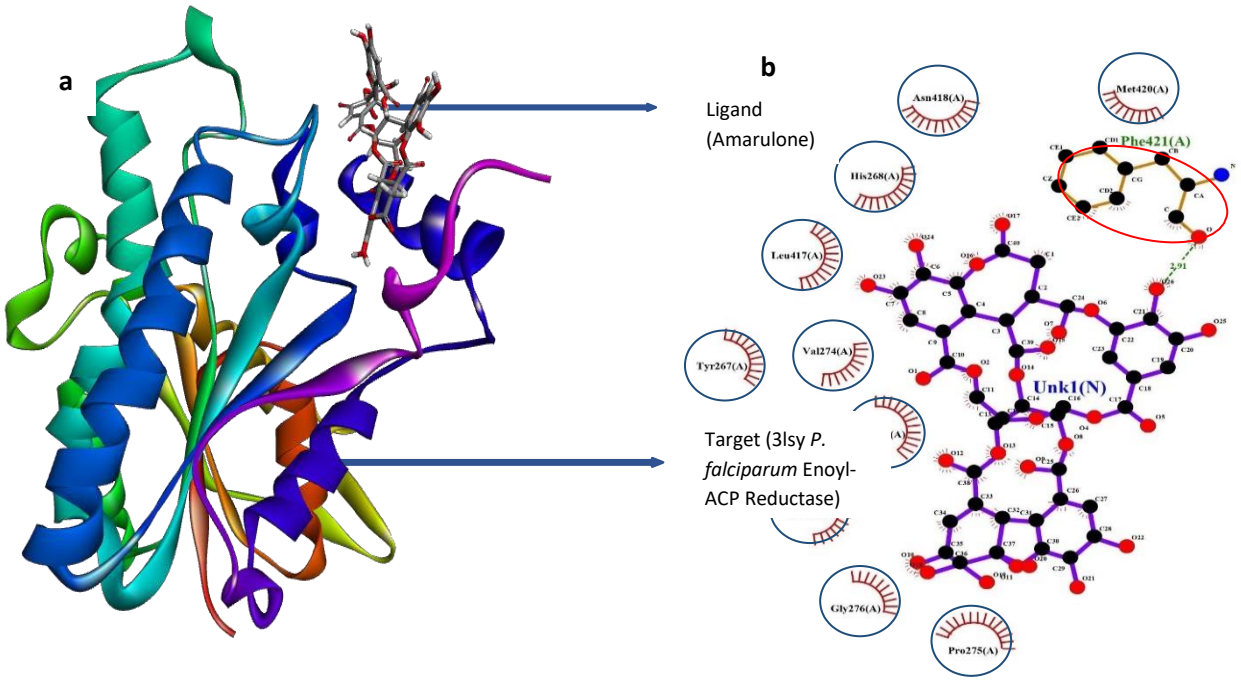

Figure 2 Amarulone-3lsy docked complex, showing interaction between the ligand and protein and the binding site residue.

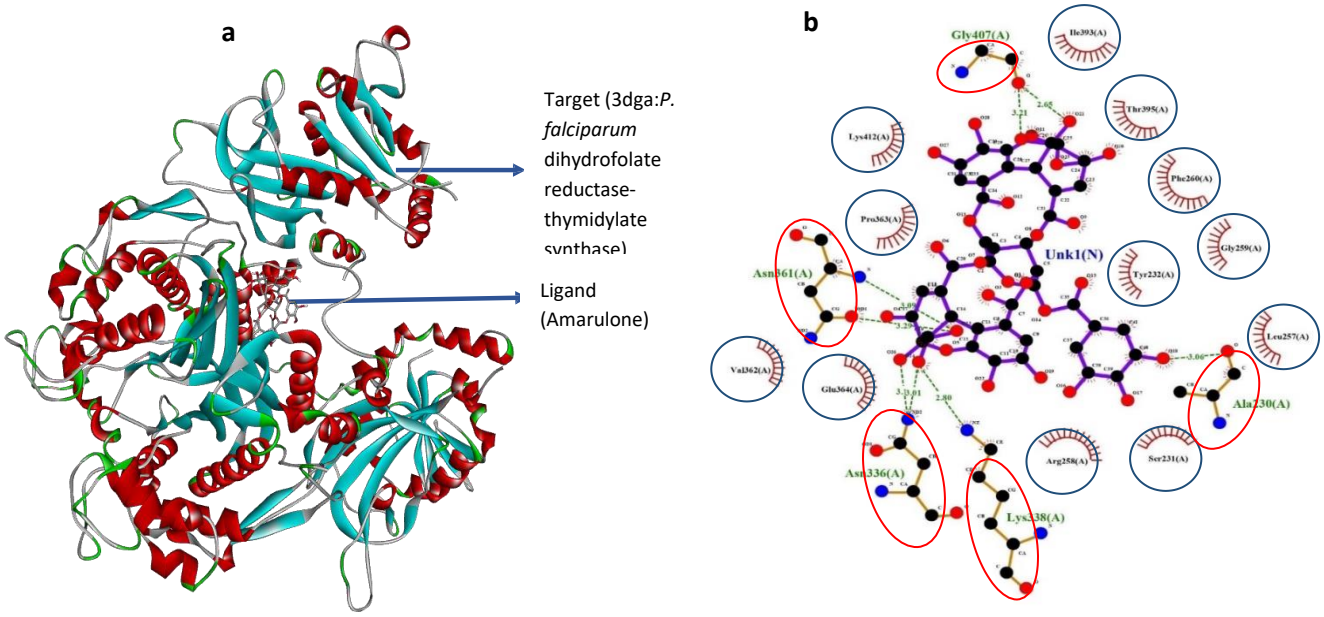

Figure 3 Amarulone-3dga docked complex, showing interaction between the ligand and protein and the binding site residue.

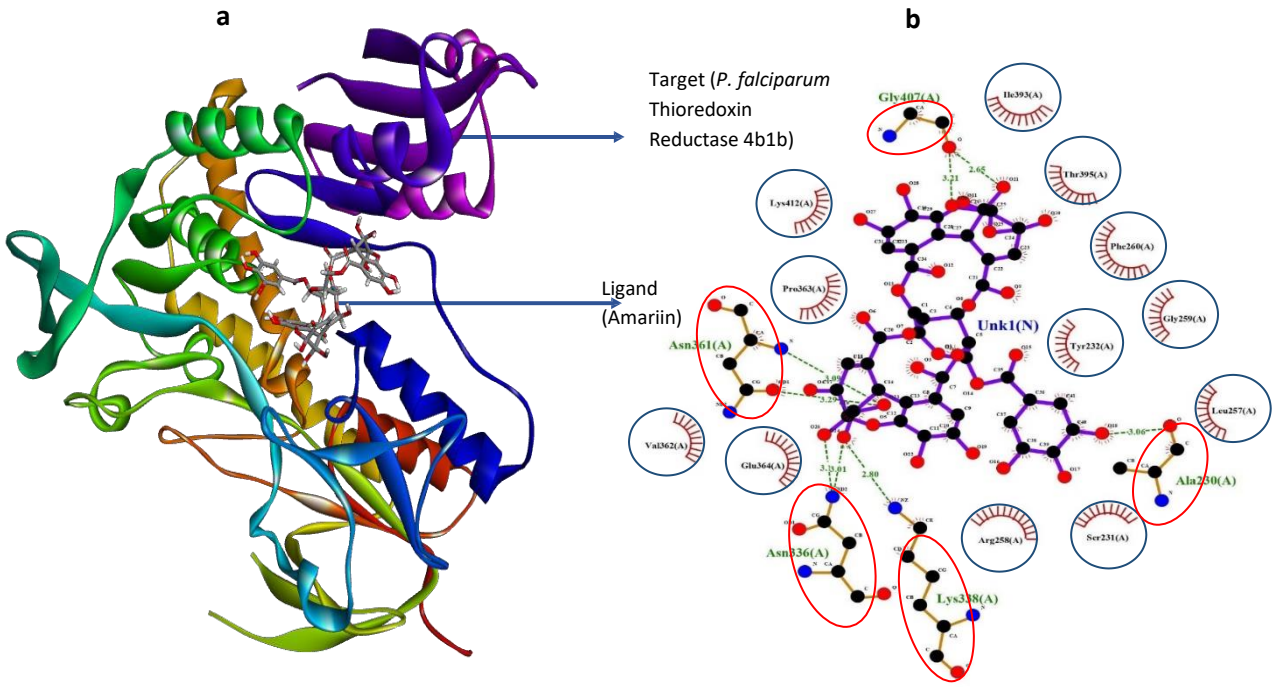

Figure 4 Amariin-4b1b docked complex, showing interaction between the ligand and protein and the binding site residue.

System Stability and Flexibility

Root Mean Square Deviation (RMSD)

The protein-ligand complex's average RMSD values for the heavy backbone atoms are 3.09 and 3.90; 1.86 and 2.02; 3.19 and 3.21; 2.26 and 3.23; 2.74 and 2.71; and 2.48 and 2.39 Å for Amariin-4b1b complex, Amarulone-1u5c complex, Amarulone-3dga complex, Amarulone-3lsy complex, Amarulone-4b1b complex and Artesunate-3sfk complex (control) respectively by finding the average of the RMSD values.

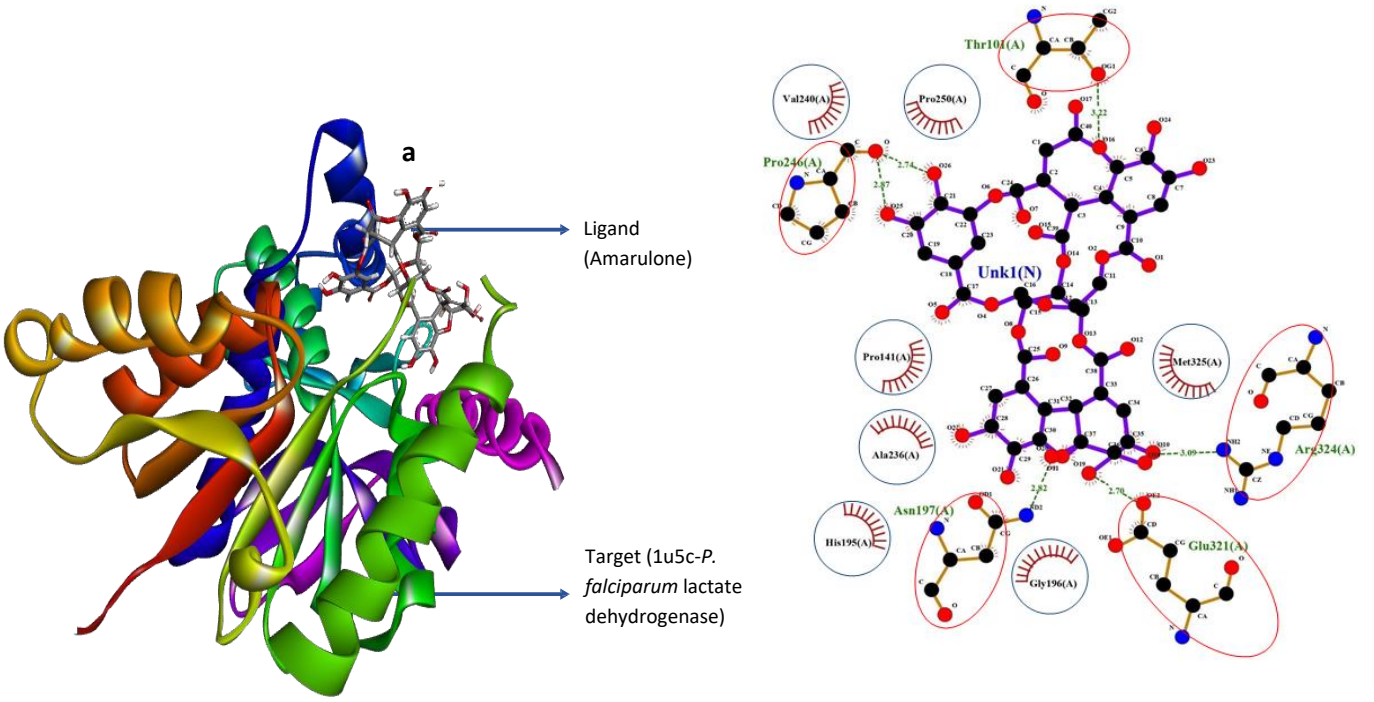

Figure 5 Amarulone-1u5c docked complex, showing interaction between the ligand and protein and the binding site residue

The diagram (a) was generated using Discovery studio v21.1, while diagram (b) was generated using LigPlot+. Unk1(N) indicate the ligand, the red ellipses indicate the amino acid residues that forms hydrogen bond(s) with the ligand and the green circles indicate amino acid residues that are in hydrophobic contact with the ligand.

Root Mean Square Fluctuation (RMSF)

The average RMSF value of the α-Carbon backbone for the simulated complexes is as follows: 1.40, 0.91, 1.60, 0.87, 1.28 and 1.04 Å for Amariin-4b1b complex, Amarulone-1u5c complex, Amarulone-3dga complex, Amarulone-3lsy complex, Amarulone-4b1b complex, and Artesunate-3sfk complex (control) respectively. Figure 7a, 7b, 7c, 7d, 7e, 7f show RMSF plots of the α-Carbon backbone for the simulated complexes.

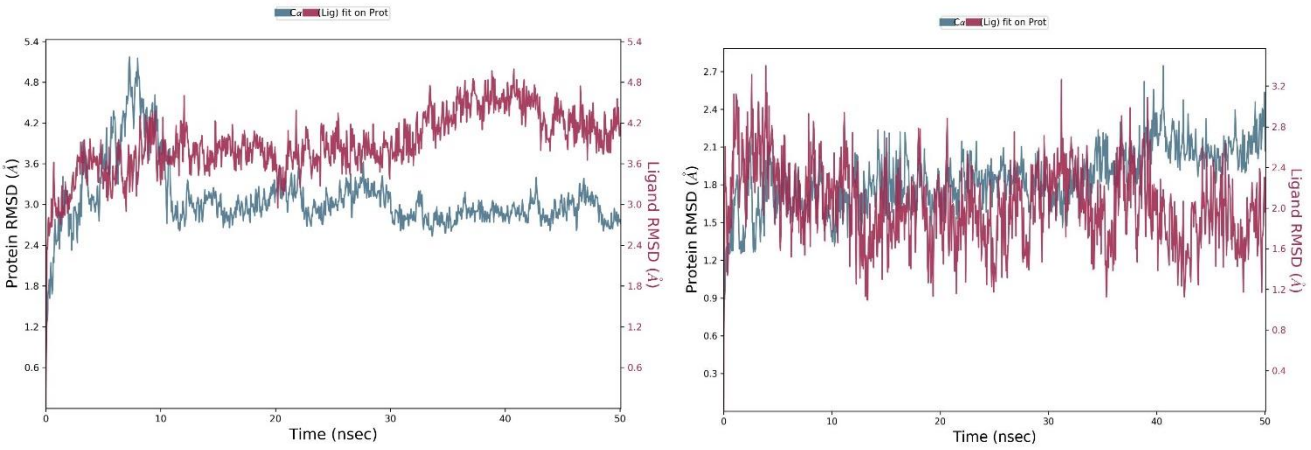

(a) (b)

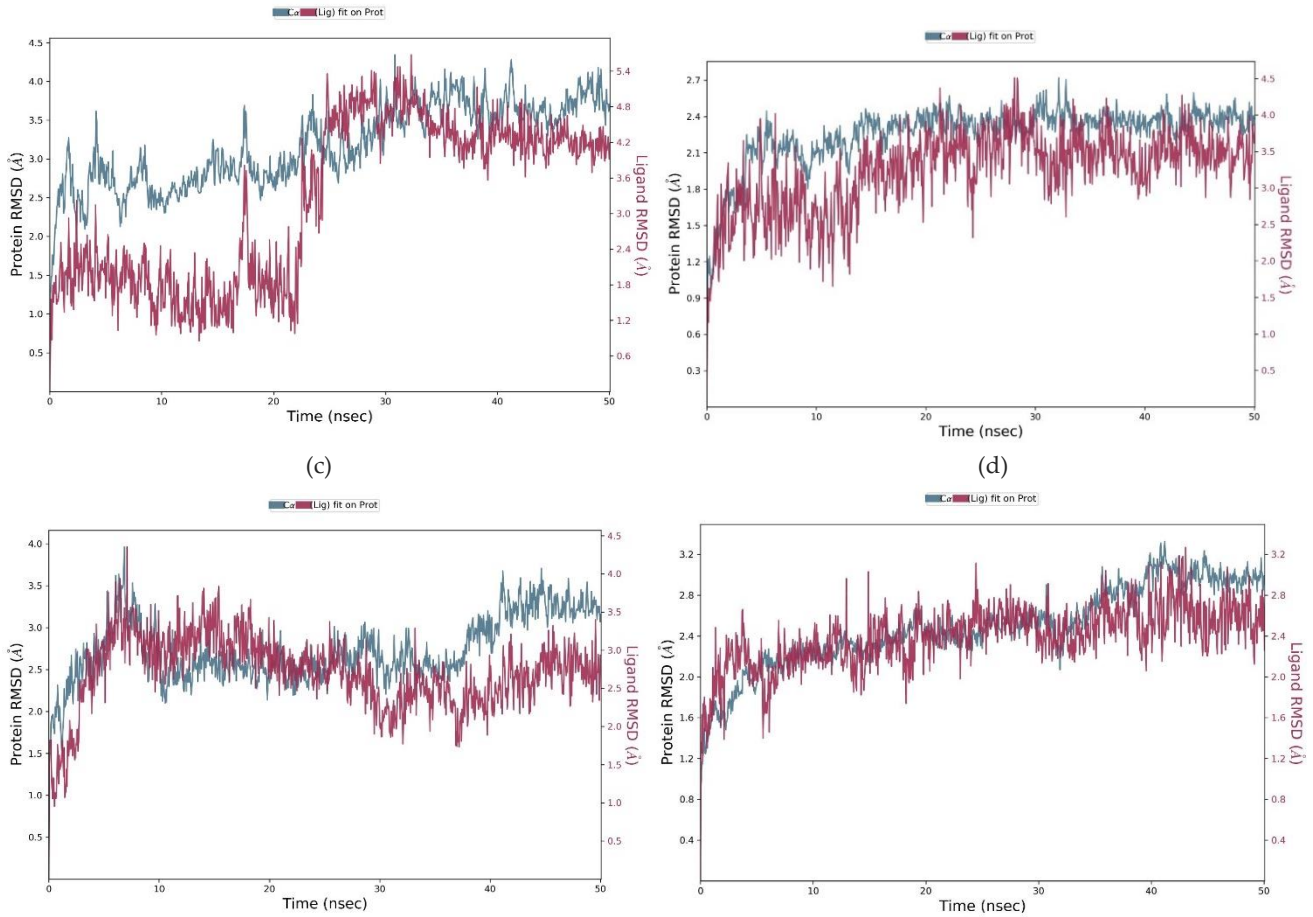

Figure 6 RMSD plots for the heavy backbone atoms of protein (C*α*) and Lig. fit Prot. of a) Amariin-4b1b complex; b) Amarulone-1u5c complex; c) Amarulone-3dga complex; d) Amarulone-3lsy complex; e) Amarulone-4b1b complex; f) Artesunate-3sfk (control)

Time (ns) was taken in X-axis and RMSD was taken in Y-axis

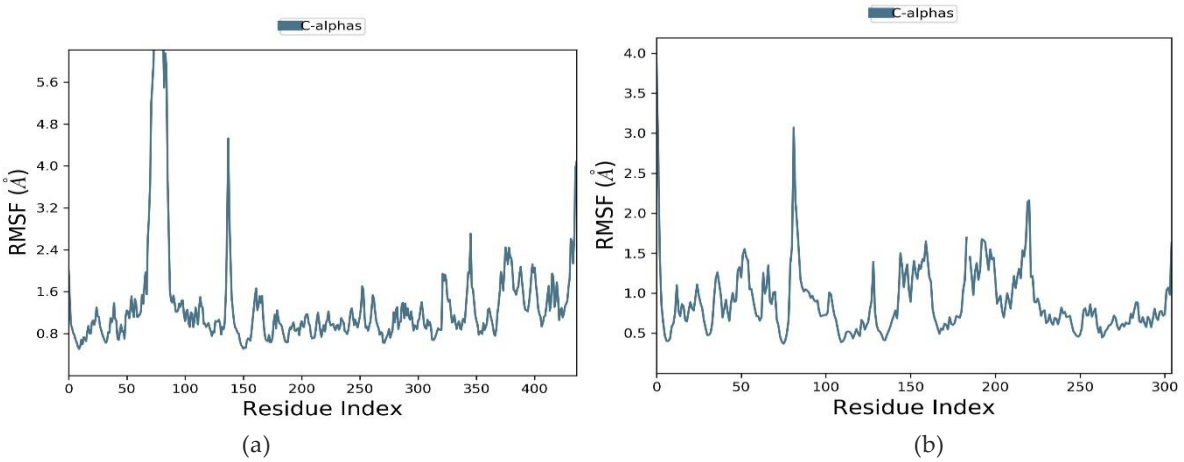

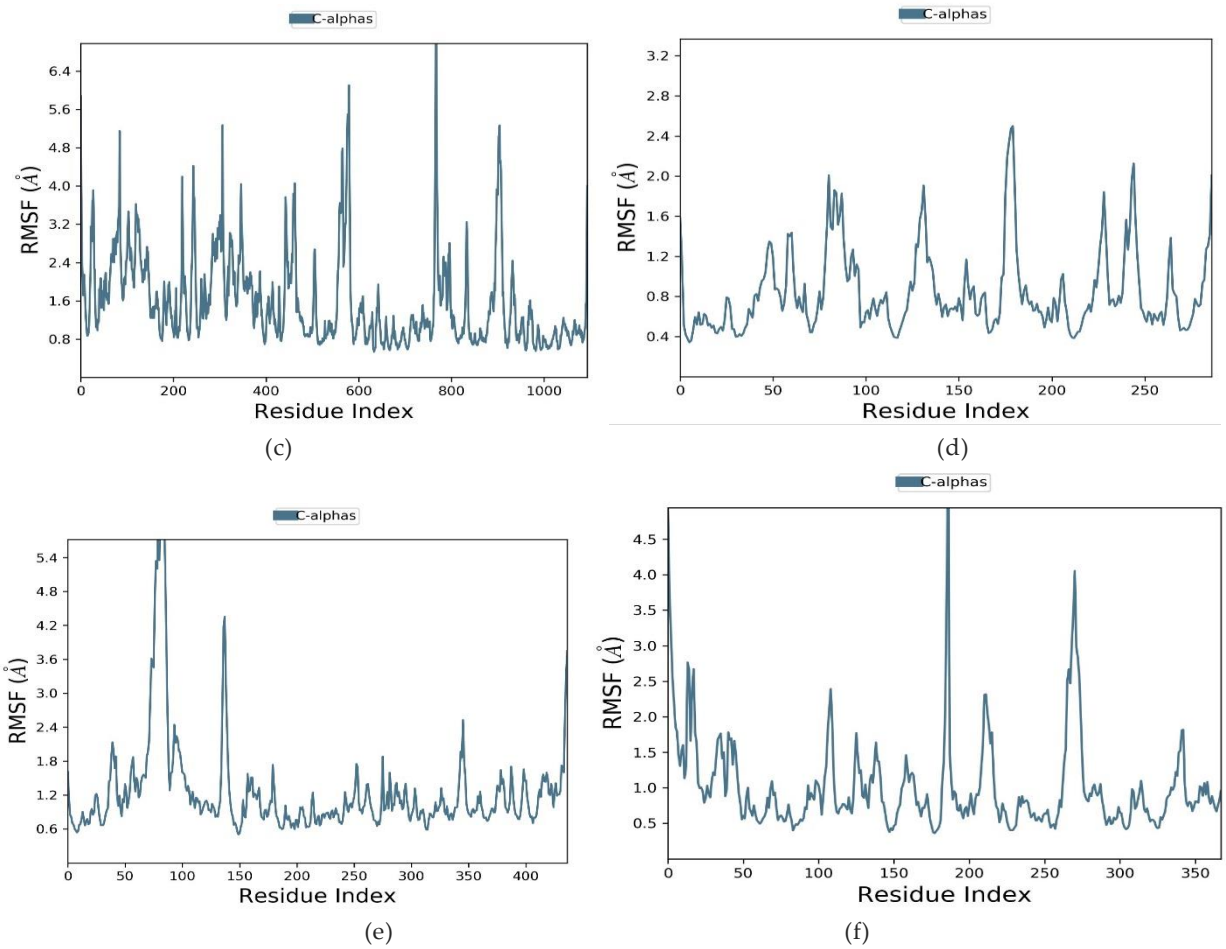

Figure 7 RMSF plot for the heavy backbone atoms of protein (Cα) of a) Amariin-4b1b; b) Amarulone-1u5c; c) Amarulone-3dga; d) Amarulone-3lsy; e) Amarulone-4b1b; f) Artesunate-3sfk (control) complex.

Residue index was taken on X-axis and RMSF was taken on Y-axis.

4. DISCUSSION

Lipinski's rule of five evaluates the drug-likeness of phytoconstituents present in plants and whether such a phytoconstituent possesses qualities that make it probable to be an oral drug in humans. A druggable compound must not violate more than one of these five rules. The molsoft web tool assigns scores to the compounds. Compounds that were assigned positive values are considered druggable. All the compounds that passed the druggability test have a high chance of being the next antimalarial drug compared to those that did not (Chen et al., 2020).

Consequently, about fifty percent of the phytocompounds analyzed using Lipinski's rule and molsoft tool were found to be lead drug candidates, especially repandusinic acid B which had the highest drug-likeness score. The ADMET prediction has two main purposes: To minimize the danger of compounds that are struck by late-stage attrition and to optimize testing and screening by focusing solely on the most promising compounds (Kar and Leszczynski, 2020). Thus, ADMET prediction plays a crucial role in the process of developing new drugs. About 40% of the compounds in this study demonstrated good ADMET profile and all the compounds passes human intestinal absorption prediction.

Among the twenty-seven compounds docked against the various plasmodial targets, Amarulone performed extremely well than the standard. This compound belongs to the class of phytochemicals called tannins and it is one of the phytoconstituents found in *Phyllanthus amarus*. To the best of our knowledge, Amarulone's antiplasmodial activity has not been documented in any literature. Meanwhile, the interaction of the compounds with the protein target must be examined to ensure that the compounds genuinely bind at the active sites in order to confirm that the best-docked compounds are real and not false positives.

Using the Ligplot+ tool, it was established that these compounds interact with the amino acid residues in the protein's active site; the nature of the interaction and the bond distance was also established. Based on the docking result and visualization of the complexes, Amarulone emerges as the most active inhibitor, forming hydrogen bonds with *Pf*TrxR at key amino residues (Asn 336, Lys338, Ile393 and Gly407) for good stability. These amino acid residues have been previously reported to be at the active site of

*Pf*TrxR (Boumis et al., 2012), allowing excellent interaction between the small molecule (phytocompounds) and the protein. Also, Amarulone had a hydrogen bond interaction with *Pf*ENR.

However, only a single amino acid residue (Phe421) is involved. This could form a weaker bond compared to the interactions between Amarulone and Amariin having multiple hydrogen bonds with various amino acid residues. Meanwhile, other amino acids, including Pro275, Gly276, Tyr267/371/375, Val274, Leu417, His268, Asn418 and Met420, form hydrophobic contact with Amarulone and may contribute to the stability of the complex as they have been previously reported to be present in the active site of *Pf*ENR by Maity et al., (2011).

Amarulone was also visualized to form hydrogen bond interactions with *Pf*DHFR-TS, involving Asn330, Tyr322, Asp212, Gln327, Tyr365 and Lys297 amino acids. Since the amino acids have reportedly been found in the active sites of PfDHFR-TS, it is anticipated that this will considerably increase the complex's stability (Dasgupta et al., 2009). Also, Amarulone exhibited hydrogen bonds with multiple amino acids of *Pf*LDH, namely Pro246, Thr101, Arg324, Glu321 and Asn197, which have been reported to be present in the active site of protein (Conners et al., 2005).

With Amarulone interacting with the amino acid residues on the active sites of these various key therapeutic targets, it is very likely to serve as a potent inhibitor. In other words, it can prevent the protein targets from interacting with their substrates. According to several previous studies, an average RMSD value < 2.0 Å corresponds to a good docking solution; a value between 2.0 and 3.0 Å deviates from the position of reference but with maintained desired orientation; and a value > 3.0 Å is completely wrong (Ramirez and Caballero, 2018).

In this study, Amarulone-1u5c (*P. falciparum* lactate dehydrogenase) complex has the lowest average RMSD value of 1.86 and 2.02 Å for the heavy backbone and protein-ligand complex respectively, while Amariin-4b1b (*P. falciparum* Thioredoxin Reductase) complex has the highest RMSD value of 3.90 Å for the protein-ligand complex and Amarulone-3dga *(P. falciparum* dihydrofolate reductase-thymidylate synthase) complex has the highest RMSD value of 3.19 Å for the heavy backbone. Based on the results Amarulone-1u5c complex is the most stable out of all the simulated complexes, even better than the control Artesunate-3sfk (*P. falciparum* dihydroorotate dehydrogenase) complex which has 2.48 and 2.39 Å for the heavy backbone atoms and protein-ligand complex.

The RMSF aids in characterizing local alterations along the protein chain, which shows how flexible the protein is on binding with ligand. Abouelela et al., (2021) claim that a higher RMSF value during MD simulation denotes greater flexibility. Hence, from the result obtained Amarulone-3dga *(P. falciparum* dihydrofolate reductase-thymidylate synthase) complex has the highest RMSF value of 1.60Å, making it the most flexible out of the simulated complexes, follow by Amariin-4b1b, Amarulone-4b1b, Amarulone-1u5c complex with RMSF value of 1.40, 1.28, 0.91 Å respectively. Amarulone-3lsy (*P. falciparum* Enoyl-ACP Reductase) complex has the lowest average RMSF value of 0.87 Å. The control complex Artesunate-3sfk has a RMSF value of 1.04 Å.

5. CONCLUSION

The phytocompounds present in *Phyllanthus amarus* showed strong inhibitory potentials against *Plasmodium falciparum* validated drug target. This is especially true for Amarulone, which has the best binding scores with *Plasmodium falciparum* lactate dehydrogenase, *P. falciparum* dihydrofolate reductase-thymidylate synthase, *P. falciparum* dihydroorotate dehydrogenase, *P. falciparum* enoyl-acyl carrier protein Reductase and *P. falciparum* thioredoxin reductase and Amariin which binds well with *P. falciparum* thioredoxin reductase. The molecular dynamics simulation also shows that Amarulone- *P. falciparum* thioredoxin reductase complex is stable.

Thus, these bioactive compounds from *Phyllanthus amarus* have strong potential and can be developed as a novel antiplasmodial agent. As far as we know, Amarulone's antiplasmodial activity has not been documented in the literature. Therefore, these promising inhibitors merit additional *in vivo* and *in vitro* biological and pharmacological studies to confirm this study's prediction and help develop a new and effective therapy against malaria.

Informed consent

Not applicable.

Ethical approval

Not applicable.

Conflicts of interests

The authors declare that there are no conflicts of interests.

Funding

The study has not received any external funding.

Data and materials availability

All data associated with this study are present in the paper.

REFERENCES AND NOTES

1. Abouelela ME, Assaf HK, Abdelhamid RA, Elkhyat ES, Sayed AM, Oszako T, Belbahri L, El-Zowalaty AE, Abdelkader MS. Identification of potential SARS-CoV-2 main protease and spike protein inhibitors from the genus Aloe: An in- silico study for drug development. Molecules 2021; 26:1767. doi: 10.3390/ molecules26061767
2. Adjene JO, Nwose EU. Histological effects of chronic administration of *Phyllanthus amarus* on the kidney of adult Wistar rat. N Am J Med Sci 2010; 2:193-195.
3. Aliyu K, Mohammed Y, Abdullahi IN, Umar AA, Bashir F, Sani MN, Kabuga AI, Adamu AY, Akande AO. *In vitro* antiplasmodial activity of *Phyllanthus amarus* against *Plasmodium falciparum* and evaluation of its acute toxicity effect in mouse model. Trop Parasitol 2021; 11(1):31–37.
4. BIOVIA. Dassault Systèmes, Discovery stuidio, Release, San Diego 2020.
5. Birnbaum J, Flemming S, Reichard N, Soares AB, Mesén-Ramírez P, Jonscher E, Spielmann T. A genetic system to study *Plasmodium falciparum* protein function. Nat Methods 2017; 14(4):450.
6. Bjørklund G, Zou L, Wang J, Chasapis CT, Peana M. Thioredoxin reductase as a pharmacological target. Pharmacol Res 2021; 174:105854.
7. Boumis G, Giardina G, Angelucci F, Bellelli A, Brunori M, Dimastrogiovanni D, Saccoccia F, Miele AE. Crystal structure of *Plasmodium falciparum* thioredoxin reductase, a validated drug target. Biochem Biophys Res Commun 2012; 425(4):806-11. doi: 10.1016/j.bbrc.2012.07.156
8. Chaniad P, Mungthin M, Payaka A, Viriyavejakul P, Punsawad C. Antimalarial properties and molecular docking analysis of compounds from *Dioscorea bulbifera* L. as new antimalarial agent candidates BMC Complement Med Ther 2021; 21:144. doi: 10.1186/s12906-021-03317-y
9. Chen X, Li H, Tian L, Li Q, Luo J, Zhang Y. Analysis of the Physicochemical Properties of Acaricides Based on Lipinski's Rule of Five. J Comput Biol 2020; 27(9):1397-1406.
10. Conners R, Schambach F, Read J, Cameron A, Sessions RB, Vivas L, Easton A, Croft SL, Brady RL. Mapping the binding site for gossypol-like inhibitors of *Plasmodium falciparum* lactate dehydrogenase. Mol Biochem Parasitol 2005; 142(2):137-48.
11. Costa-Júnior DB, Araújo JSC, Oliveira LM, Neri FSM, Moreira POL, Taranto AG, Fonseca AL, Varotti FP, Leite FHA. A novel antiplasmodial compound: Integration of in silico and in vitro assays. J Biomol Struct Dyn 2022; 40(14):6295-6307. doi: 10.1080/07391102.2021.1882339
12. Dallakyan S, Olson AJ. Small-molecule library screening by docking with PyRx. Methods Mol Biol 2015; 1263:243-250.
13. Dasgupta T, Chitnumsub P, Kamchonwongpaisan S, Maneeruttanarungroj C, Nichols SE, Lyons TM, Tirado-Rives J, Jorgensen WL, Yuthavong Y, Anderson KS. Exploitingstructural analysis, *in silico* screening and serendipity to identify novel inhibitors of drug-resistant *falciparum* malaria. ACS Chem Biol 2009; 4(1):29-40.
14. Desai TH, Joshi SV. *In silico* evaluation of apoptogenic potential and toxicological profile of triterpenoids. Indian J Pharmacol 2019; 513:181-207.
15. Donkor AM, Mensah DO, Ani E, Ankamah E, Nsiah S, Mensah DE. In vitro anti-plasmodial activity of aqueous and ethanolic extracts of *Moringa oleifera* and *Phyllanthus amarus.* Int J Biol Chem 2015; 9:198–206.
16. Elabbadi N, Ancelin ML, Vial HJ. Use of radioactive ethanolamine incorporation into phospholipids to assess in vitro antimalarial activity by the semi-automated microdilution technique. Antimicrob Agents Chemother 1992; 36:50-55.
17. Etta H. Effects of *Phyllanthus amarus* on litter traits in albino rats. Sci Res Essays 2008; 38:370–372.
18. Harder E, Damm W, Maple J, Wu C, Reboul M, Xiang JY, Wang L, Lupyan D, Dahlgren MK, Knight JL, Kaus KW, Cerutti DS, Krilov G, Jorgensen WL, Abel R, Friesner RA. OPLS3: A force field providing broad coverage of drug-like small molecules and proteins. J Chem Theory Comput 2016; 12:281-296.
19. Hoelz LV, Calil FA, Nonato MC, Pinheiro LC, Boechat N. *Plasmodium falciparum* dihydroorotate dehydrogenase: A drug target against malaria. Future Med Chem 2018; 10(15):1853–1874.

20. Jortzik E, Becker K. Thioredoxin and glutathione systems in *Plasmodium falciparum.* Int J Med Microbiol 2012; 3024-5:187-94.
21. Kar S, Leszczynski J. Open access in silico tools to predict the ADMET profiling of drug candidates. Expert Opin Drug Discov 2020; 15(12):1473-1487.
22. Laskowski RA, Swindells MB. LigPlot+: Multiple ligand-protein interaction diagrams for drug discovery. J Chem Inf Model 2011; 51(10):2778–2786.
23. Lipinski CA. Lead- and drug-like compounds: The rule-of five revolution. Drug Discov Today Technol 2004; 1(4):337e41.
24. Maity K, Banerjee T, Prabakaran N, Surolia N, Surolia A, Suguna K. Effect of substrate binding loop mutations on the structure, kinetics and inhibition of enoyl acyl carrier protein reductase from *Plasmodium falciparum*. IUBMB Life 2011; 63(1):30-41. doi: 10.1002/iub.412
25. Makenga G, Menon S, Baraka V, Minja DTR, Nakato S, Delgado-Ratto C, Francis F, Lusingu JPA, Geertruyden JP. Prevalence of malaria parasitaemia in school-aged children and pregnant women in endemic settings of sub-Saharan Africa: A systematic review and meta-analysis. Parasite Epidemiol Control 2020; 11:e00188.
26. Mohanraj K, Karthikeyan BS, Vivek-Ananth RP, Chand RPB, Aparna SR, Mangalapandi P, Samal A. IMPPAT: A curated database of Indian Medicinal Plants, Phytochemistry and Therapeutics. Sci Rep 2018; 8:4329.
27. Mosquera-Yuqui F, Lopez-Guerra N, Moncayo-Palacio EA. Targeting the 3CLpro and RdRp of SARS-CoV-2 with phytochemicals from medicinal plants of the Andean Region: Molecular docking and molecular dynamics simulations. J Biomol Struct Dyn 2022; 40(5):2010-2023.
28. Narayanaswamy R, Wai LK, Ismail IS. Natural Compounds as Inhibitors of *Pf*ENR; An *in-silico* Study. J Chosun Nat Sci 2017; 101:1-6.
29. O'Keefe JD, Dustin CM, Barber DR, Snider GW, Hondal RJ. A 'Seleno Effect' Differentiates the Roles of Redox Active Cysteine Residues in *Plasmodium falciparum* Thioredoxin Reductase. Biochemistry 2018; 57(11):1767–1778.
30. Pettersen EF, Goddard TD, Huang CC, Couch GS, Greenblatt DM, Meng EC, Ferrin TE. UCSF Chimera—a visualization system for exploratory research and analysis. J Comput Chem 2004; 25(13):1605-1612.
31. Qidwai T, Khan F. Antimalarial drugs and drug targets specific to fatty acid metabolic pathway of *Plasmodium falciparum.* Chem Biol Drug Des 2012; 80:155-172.
32. Ralph SA, Dooren GG, Waller RF, Crawford MJ, Fraunholz MJ, Foth BJ, Tonkin CJ, Roos DS, Mc-Fadden GI. Tropical infectious diseases: Metabolic maps and functions of the *Plasmodium falciparum* apicoplast. Nat Rev Microbiol 2004; 2:203-216.
33. Ramirez D, Caballero J. Is it reliable to take the molecular docking top scoring position as the best solution without considering available structural data? Molecules 2018; 23:1038. doi: 10.3390/molecules23051038
34. Rout S, Mahapatra RK. In silico analysis of *Plasmodium falciparum* CDPK5 protein through molecular modeling, docking and dynamics. J Theor Biol 2019; 461:254-267.
35. Shadrack DM, Nyandoro SS, Munissi JJE, Mubofu EB. In Silico Evaluation of Anti-Malarial Agents from *Hoslundia opposita* as Inhibitors of *Plasmodium falciparum* Lactate Dehydrogenase (PfLDH) Enzyme. Comput Mol Biosci 2016; 6:23–32. doi: 10.4236/CMB.2016.62002
36. Sharma VL, Abbat S, Bharatam PV. Pharmacoinformatic Study on the Selective Inhibition of the Protozoan Dihydrofolate Reductase Enzymes. Mol Inform 2017; 36(11):1600156–1600156.
37. Singh IV, Mishra S. Molecular Docking Analysis of Pyrimethamine Derivatives with *Plasmodium falciparum* Dihydrofolate Reductase. Bioinformation 2018; 14(5):232–235.
38. Vaughan AM, O'Neill MT, Tarun AS, Camargo N, Phuong TM, Aly AS, Cowman AF, Kappe SH. Type II fatty acid synthesis is essential only for malaria parasite late liver stage development. Cell Microbiol 2009; 11(3):506-20. doi: 10.1111/j.1462-5822.2008.01270.x
39. Yang H, Lou C, Sun L, Li J, Cai Y, Wang Z. admetSAR 2.0: Web-service for prediction and optimization of chemical ADMET properties. Bioinformatics 2019; 356:1067-1069.